

The Bethe-Salpeter approach to bound states: from Euclidean to Minkowski space.

A. Castro^a, E. Ydrefors^a, W. de Paula^a, T. Frederico^a, J.H. de Alvarenga Nogueira^{a,b}, P. Maris^c

^aInstituto Tecnológico da Aeronáutica, DCTA, 12.228-900 São José dos Campos, SP, Brazil

^bUniversità di Roma La Sapienza, INFN, Sezione di Roma, P.le A. Moro 5, 00187 Roma, Italy

^cDepartment of Physics and Astronomy, Iowa State University, Ames, IA 50011, USA

Abstract. The challenge to obtain from the Euclidean Bethe-Salpeter amplitude the amplitude in Minkowski is solved by resorting to un-Wick rotating the Euclidean homogeneous integral equation. The results obtained with this new practical method for the amputated Bethe-Salpeter amplitude for a two-boson bound state reveals a rich analytic structure of this amplitude, which can be traced back to the Minkowski space Bethe-Salpeter equation using the Nakanishi integral representation. The method can be extended to small rotation angles bringing the Euclidean solution closer to the Minkowski one and could allow in principle the extraction of the longitudinal parton density functions and momentum distribution amplitude, for example.

1. Introduction

Techniques to solve the Bethe-Salpeter Equation (BSE) in Minkowski space have been developed for bound state of bosons [1, 2, 3, 4, 5] and fermions [6, 7, 8], at the expense of being algebraically quite involved, either by use of the Nakanishi integral representation (NIR) [9] or by direct integration. On the other hand, calculations done in Euclidean space after performing the Wick rotation of the BSE are conceptually straightforward [10, 11], but it is nontrivial to obtain structure observables that are defined on the light-front, such as e.g. parton distributions, from Euclidean solutions. It is desirable to be able to undo the Wick rotation and obtain the Minkowski space solutions from the Euclidean solutions, such that one could extract Minkowski space observables. The first steps in this direction are provided in this contribution.

Our goal here is to present solutions of the BSE for two-bosons close to the Minkowski space, by introducing a rotation into the complex plane of $k_0 \rightarrow k_0 \exp(i\theta)$, where $\theta = \pi/2$ is the standard Wick-rotation associated with the Euclidean space formulation, while the Minkowski space formulation corresponds to $\theta = 0$. We present solutions of the BSE for small angles and show that the rich analytic structure is accessible numerically by such technique [12]. The branch-points obtained from the integral representation of the vertex function are exhibited by our accurate numerical solutions, for the two-boson bound state in ladder approximation. We present an initial study with angles small as $\theta = \pi/128 \approx 1.4^\circ$, where we also explore different masses μ of the exchanged boson, as well as binding energies.

2. Two-body BSE in Euclidean space

A two-body bound state with total four-momentum p with $p^2 = -M^2$ can be described by the amputated Bethe–Salpeter vertex function Γ , which is a solution of the two-body bound state equation

$$\Gamma(k^2, k \cdot p; p^2 = -M^2) = \int \frac{d^4 k'}{(2\pi)^4} K(k - k'; p) \Delta(\frac{p}{2} + k') \Gamma(k'^2, k' \cdot p; p^2 = -M^2) \Delta(\frac{p}{2} - k'). \quad (1)$$

Here, K is the two-body scattering kernel, and Δ are the (dressed) propagators for the constituent particles. In ladder truncation, the kernel reduces to $\frac{g^2}{(k-k')^2 + \mu^2}$. Using bare propagators in the rest frame with 3-dimensional spherical coordinates, $p = (iM, \vec{p} = 0)$, we have for the scalar bound state in the Euclidean metric

$$\begin{aligned} \Gamma(k_0, k_v; iM) &= -\frac{m^2 \alpha}{\pi^2} \int_{-\infty}^{+\infty} dk'_0 \int_0^{+\infty} dk'_v \frac{k'_v}{k_v} \ln \left(\frac{(k_0 - k'_0)^2 + (k_v - k'_v)^2 + \mu^2}{(k_0 - k'_0)^2 + (k_v + k'_v)^2 + \mu^2} \right) \\ &\times \frac{\Gamma(k'_0, k'_v; iM)}{[(\frac{i}{2}M + k'_0)^2 + k'^2_v + m^2] [(\frac{i}{2}M - k'_0)^2 + k'^2_v + m^2]}, \end{aligned} \quad (2)$$

where $k_v \equiv |\vec{k}_v|$ and $k'_v \equiv |\vec{k}'_v|$, and $\alpha = g^2/(16\pi m^2)$. The corresponding canonical normalization condition [13] can be written as

$$N^2 = \frac{1}{4\pi^3} \int_{-\infty}^{+\infty} dk_0 \int_0^{+\infty} dk_v \frac{k_v^2 [\Gamma(k_0, k_v; iM)]^2}{[(\frac{i}{2}M + k_0)^2 + k_v^2 + m^2]^2 [(\frac{i}{2}M - k_0)^2 + k_v^2 + m^2]} \quad (3)$$

such that $\Gamma(k_0, k_v; iM)/N$ is the properly normalized amputated Bethe–Salpeter vertex.

Although BSE is usually solved in the rest frame of the bound state, it should be noted that the (amputated) vertex $\Gamma(k^2, k \cdot p; p^2 = -M^2)$ is a function of the Lorentz scalar variables k^2 and $k \cdot p$ at fixed p^2 . As long as the truncation of the BSE does not break Lorentz invariance (including any regularization schemes of divergences), the obtained solution is frame independent, and therefore does not need to be boosted for e.g. form factor calculations. Indeed, it has been demonstrated that meson observables, including form factors, calculated in the ladder truncation, are indeed frame-independent [14, 15].

3. Un-Wick rotation towards Minkowski space

Starting with the Euclidean space ladder BSE the rest frame, Eq. (2), we can make a change of variables $k_0 \rightarrow k_0 e^{i\delta}$ and $k'_0 \rightarrow k'_0 e^{i\delta}$ with the rotation angle $\delta = \theta - \pi/2$, where θ is the rotation angle with respect to the usual Minkowski definition of the zero component of the momentum. Thus the un-Wick rotated BSE becomes

$$\begin{aligned} \Gamma(e^{i\delta} k_0, k_v; iM) &= -\frac{m^2 \alpha e^{i\delta}}{\pi^2} \int_{-\infty}^{+\infty} dk'_0 \int_0^{+\infty} dk'_v \frac{k'_v}{k_v} \ln \left(\frac{e^{2i\delta} (k_0 - k'_0)^2 + (k_v - k'_v)^2 + \mu^2}{e^{2i\delta} (k_0 - k'_0)^2 + (k_v + k'_v)^2 + \mu^2} \right) \\ &\times \frac{\Gamma(e^{i\delta} k'_0, k'_v; iM)}{[(\frac{i}{2}M + e^{i\delta} k'_0)^2 + k'^2_v + m^2] [(\frac{i}{2}M - e^{i\delta} k'_0)^2 + k'^2_v + m^2]}, \end{aligned} \quad (4)$$

which can be solved numerically, e.g. by iteration. In particular, starting from the Euclidean solution ($\delta = 0$), one can increase δ in small steps, and at each step use the solution at the previous step as the initial guess for solving the BSE iteratively, as is illustrated in the left panel of Fig. 1. Of course, as one approaches the Minkowski axis ($\delta \rightarrow \pi/2$, or equivalently, $\theta \rightarrow 0$), the numerical challenges in order to obtain a stable solution increase. Although we cannot solve the BSE at $\theta = 0$ exactly, we may be able to extrapolate to $\theta = 0$.

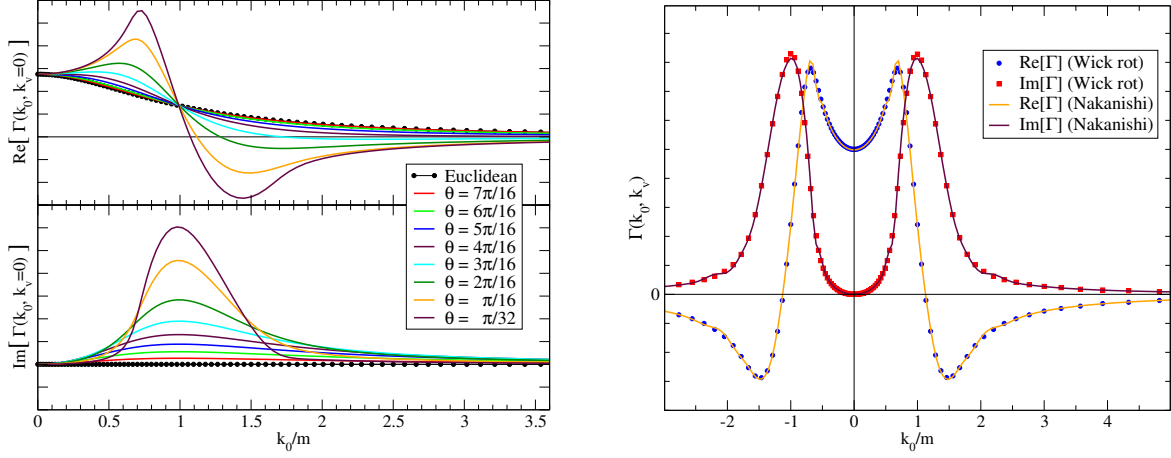


Figure 1. Numerical solutions for $\Gamma(k_0, k_v)$ for $\mu/m = 0.2$ and $M/m = 1.0$ in arbitrary units. Left: Solutions of the un-Wick rotated Euclidean BSE for a range of θ ; Right: Comparison of the un-Wick rotated Euclidean BSE and the NIR at $\theta = \pi/16 \approx 11^\circ$.

4. Two-body BSE in Minkowski space

Alternatively, one can use the NIR to solve the BSE in Minkowski space formulation. Following Ref. [1], we make use of the uniqueness assumption of the Nakanishi weight function in the non-perturbative domain. We have to remind that for the Bethe–Salpeter amplitude itself, the uniqueness assumption can be overcome, using the method of Light-Front projection [16], followed by the application of the inverse generalized Stieltjes transform [17].

The integral representation of the vertex function Γ is

$$\Gamma(k^2, k \cdot p; p^2 = M^2) = \int_{-1}^{+1} dz \int_{\gamma_{\min}}^{\infty} d\gamma \frac{g_{\Gamma}(\gamma, z)}{\gamma + m^2 - \frac{p^2}{4} - k^2 - k \cdot p z - i\epsilon}. \quad (5)$$

A task we have to undertake is to determine the minimum value of γ by checking for the adequacy of the solution in the form above for the BSE, which can in principle depend on z [18]. After introducing the one-boson exchange kernel in the BSE, and using uniqueness, we find that [1]

$$g_{\Gamma}(\gamma, z) = \frac{g^2}{(4\pi)^2} \int_{-1}^{+1} dz' \int_0^1 d\alpha_2 \int_0^1 d\alpha_3 \frac{(1 - \alpha_3)}{(1 + z') \bar{s}} \theta(\bar{s}) \theta(1 - \bar{\alpha}) \theta(\bar{\alpha}) \theta(\gamma_0 - \gamma_{\min}) \left. \frac{\partial g_{\Gamma}(\gamma', z')}{\partial \gamma'} \right|_{\gamma' = \gamma_0},$$

where

$$\begin{aligned} \bar{s} &= \frac{(1 + z) + 2z'(\alpha_2 + \alpha_3) + \alpha_3(1 - z)}{1 + z'} \\ \bar{\alpha} &= \frac{\alpha_2(1 - z') + (z' - z)(1 - \alpha_3)}{1 + z'} \\ \gamma_0 &= \frac{\alpha_3(1 - \alpha_3)\gamma - (1 - \alpha_3)^2 \left(m^2 + (z^2 - 1) \frac{p^2}{4} \right) - \alpha_3 \mu^2}{\bar{s}} \\ \gamma_{\min} &= \mu \left(2\sqrt{m^2 + (z^2 - 1) \frac{p^2}{4}} + \mu \right). \end{aligned}$$

After a redefinition of the parameter γ , the integral equation for $g_{\Gamma}(\gamma, z)$ can be solved numerically using basis expansion (see e.g. [19]), and from that the observables like parton distributions can be calculated.

As a consistency check, we can also apply the (un-)Wick rotation to the NIR, and calculate the vertex function $\Gamma(e^{i\theta}k_0, k_v; M)$ from $g_\Gamma(\gamma, z)$. We do indeed find good agreement between the un-Wick rotated solution of the Euclidean BSE and the solution at arbitrary angles θ from the NIR, as can be seen in the right panel of Fig. 1.

5. Analytic structure of the Bethe–Salpeter amplitude

Our numerical solutions shown in the left panel of Fig. 1 strongly suggest the existence of singularities in the amputated vertex function Γ . A detailed analysis of the NIR, Eq. (5), shows that there are indeed branch-points in the amputated vertex function, located for $z = \pm 1$ at

$$\gamma_{\min} + m^2 - \frac{p^2}{4} - k^2 \pm k \cdot p = (m + \mu)^2 - \frac{p^2}{4} - k^2 \pm k \cdot p = 0, \quad (6)$$

which in the rest frame gives the branch-points at

$$|k_0| = k_0^\pm \equiv \sqrt{(m + \mu)^2 + k_v^2} \pm \frac{M}{2}. \quad (7)$$

The positive and negative branch-points in k_0 closest to the origin are separated by $2\sqrt{(m + \mu)^2 + k_v^2} - M$, which allows the rotation of the arguments of the vertex function in the complex k_0 plane without crossing singularities. This non-analytic behavior of the vertex function at these branch-points should be corroborated by the numerical results found for $\Gamma(k; p)$ in the k_0 plane.

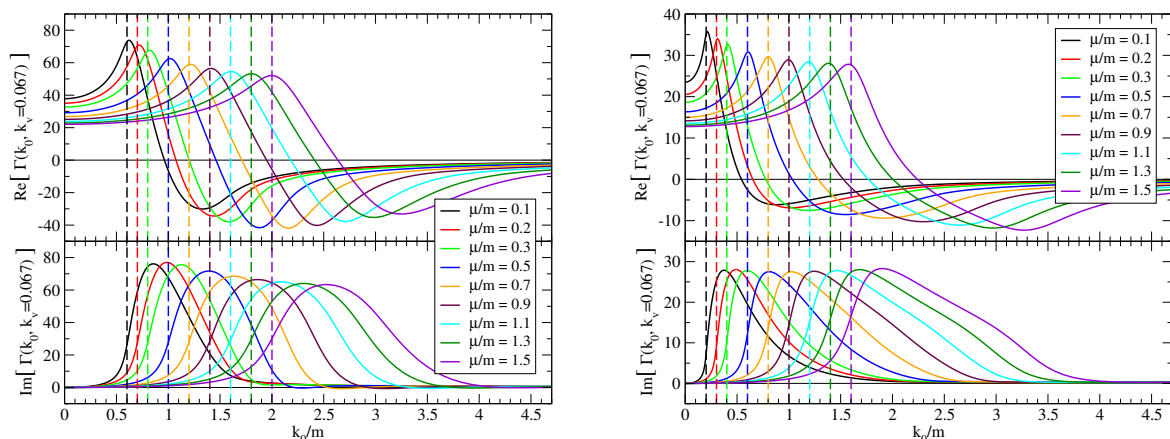


Figure 2. Numerical solutions for $\Gamma(k_0, k_v)$ at $\theta = \pi/32 \approx 5.6^\circ$ for a range of exchange masses μ . Left: for moderate binding, $M/m = 1.0$. Right: for weak binding, $M/m = 1.8$. The dashed vertical lines indicate the location of the first branch-point in $\Gamma(k_0, k_v)$.

In Fig. 2, we present our results with $0.1 \leq \mu/m \leq 1.5$ at an angle $\theta = \pi/32 \approx 5.6^\circ$ for two different bound state masses: $M/m = 1$, corresponding to moderate binding, and $M/m = 1.8$, corresponding to weak binding. The vertical bars show the location of the branch-points k_0^- , see Eq. (7), in the limit $\theta \rightarrow 0$. For $\theta = \pi/32 \approx 5.6^\circ$ the real part of $\Gamma(k_0, k_v)$ has a peak for $|k_0| \approx k_0^-$. Furthermore, the imaginary part of $\Gamma(k_0, k_v)$ is (almost) zero for $|k_0| < k_0^-$, but rises sharply near for $|k_0| \approx k_0^-$. At fixed binding energy, these peaks are more pronounced as the mass of the exchange particle decreases to zero.

As one decreases the angle θ to approach the Minkowski axis, both the peak in the real part of $\Gamma(k_0, k_v)$ and the sharp rise in the imaginary part of $\Gamma(k_0, k_v)$ become more pronounced, see

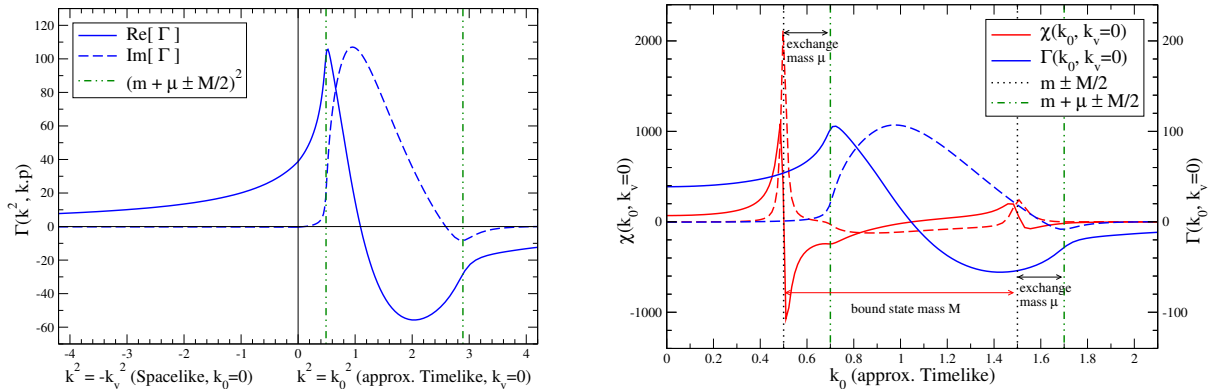


Figure 3. Numerical solution of the BSE for $\mu/m = 0.2$ and $M/m = 1.0$ at $\theta = \pi/128 \approx 1.4^\circ$. Left: $\Gamma(k^2, k \cdot p)$ as function of k^2 in both the spacelike and (approximate) timelike region; Right: results for both Γ (blue) and $\chi = \Delta\Gamma\Delta$ (red) as function of k_0 .

the left panel of Fig. 3, suggesting that this is indeed a branch-point. These high-precision numerical calculations also confirm that there are no singularities closer to $k_0 = 0$ in $\Gamma(k_0, k_v)$ than those at $|k_0| = k_0^-$. Furthermore, the kink in both the real and the imaginary parts of $\Gamma(k_0, k_v)$ indicate the location of the non-analytic points at $|k_0| = k_0^+$.

Finally, in the right panel of Fig. 3 we show the Bethe–Salpeter amplitude with the external propagator legs

$$\chi(k_0, k_v; p) = \Delta(\frac{p}{2} + k') \Gamma(k_0, k_v; p) \Delta(\frac{p}{2} - k), \quad (8)$$

in addition to $\Gamma(k_0, k_v; p)$. Here we clearly see that the analytic structure of $\chi(k_0, k_v; p)$ is dominated by the poles in the constituent propagators Δ ; the additional non-analytic structure at $|k_0| = k_0^-$ is reduced to relatively minor kinks in the real and imaginary parts of $\chi(k_0, k_v; p)$ at $|k_0| = k_0^-$, and the non-analyticity of $\chi(k_0, k_v; p)$ at $|k_0| = k_0^+$ is not even visible in this plot.

6. Concluding remarks

In this work we present a method to solve the BSE for two-bosons close the timelike axis in Minkowski space. To this end we perform an un-Wick rotation of the Euclidean BSE into the k_0 complex plane. Our solutions of this un-Wick rotated BSE are in good agreement with solutions obtained by solving the BSE in Minkowski space using the Nakanishi Integral Representation and a posteriori rotation into the complex plane. The numerical solutions suggest the existence of branch-points as one approaches the timelike region. Indeed, a detailed analysis of the Minkowski space Bethe–Salpeter equation using the Nakanishi Integral Representation reveals a rich analytic structure of the Bethe–Salpeter amplitude.

In conclusion, the un-Wick rotation captures the main physics of the vertex function, and it can be a valuable tool in the study of the Bethe–Salpeter amplitude close to the timelike region. We expect that this method can be useful to obtain structure observables that are defined on the light-front, such as e.g. parton distributions, and to further explore the phenomenology of strongly relativistic bound state systems.

Acknowledgments

We thank FAPESP Thematic grants no. 13/26258-4 and no. 17/05660-0. PM thanks the Visiting Researcher Fellowship from FAPESP, grant no. 2017/19371-0; EY thanks FAPESP grant no. 2016/25143-7; JHAN thanks FAPESP grant no. 2014/19094-8; TF thanks Conselho

Nacional de Desenvolvimento Científico e Tecnológico (Brazil) and Project INCT-FNA Proc. No. 464898/2014-5. This study was financed in part by CAPES - Finance Code 001.

References

- [1] K. Kusaka and A. G. Williams, Phys. Rev. D **51** (1995) 7026.
- [2] K. Kusaka, K. Simpson and A. G. Williams, Phys. Rev. D **56** (1997) 5071.
- [3] V. Sauli and J. Adam, Nucl. Phys. A **689** (2001) 467.
- [4] T. Frederico, G. Salmè and M. Viviani, Phys. Rev. D **85** (2012) 036009.
- [5] R. Pimentel, W. de Paula, Few Body Syst. **57** (2016) 7, 491.
- [6] J. Carbonell, V.A. Karmanov, Eur. Phys. J. A **46** (2010) 387.
- [7] W. de Paula, T. Frederico, G. Salmè, M. Viviani, Phys. Rev. D **94** (2016) 071901.
- [8] W. de Paula, T. Frederico, G. Salmè, M. Viviani, R. Pimentel, Eur. Phys. J. C **77** (2017) 11, 764.
- [9] N. Nakanishi, Suppl. Prog. Theor. Phys. **43** (1969) 1.
- [10] P. Maris and C. D. Roberts, Phys. Rev. C **56** (1997) 3369.
- [11] P. Maris and C. D. Roberts, Int. J. Mod. Phys. E **12** (2003) 297.
- [12] A. Castro *et al*, in preparation.
- [13] Claude Itzykson and Jean-Bernard Zuber, Quantum Field Theory (McGraw-Hill, 1985)
- [14] P. Maris and P. C. Tandy, Nucl. Phys. Proc. Suppl. **161** (2006) 136.
- [15] M. S. Bhagwat and P. Maris, Phys. Rev. C **77** (2008) 025203.
- [16] V. A. Karmanov and J. Carbonell, Eur. Phys. J. A **27** (2006) 1.
- [17] J. Carbonell, T. Frederico and V. A. Karmanov, Phys. Lett. B **769**, 418 (2017).
- [18] G. Wanders, Helvetica Physica Acta **30** (1957) 417.
- [19] T. Frederico, G. Salmè and M. Viviani, Phys. Rev. D **89** (2014) 016010.